



# Chamber studies of SOA formation from aromatic hydrocarbons: observation of limited glyoxal uptake

S. Nakao<sup>1,2</sup>, Y. Liu<sup>1,2,3</sup>, P. Tang<sup>1,2</sup>, C.-L. Chen<sup>1,2</sup>, J. Zhang<sup>3,4</sup>, and D. R. Cocker III<sup>1,2</sup>

<sup>1</sup>University of California, Riverside, Department of Chemical and Environmental Engineering, Riverside, USA

<sup>2</sup>College of Engineering – Center for Environmental Research and Technology (CE-CERT), Riverside, USA

<sup>3</sup>University of California, Riverside, Department of Chemistry, Riverside, USA

<sup>4</sup>University of California, Riverside, Air Pollution Research Center, Riverside, USA

Correspondence to: D. R. Cocker III (dcocker@engr.ucr.edu)

Received: 17 October 2011 – Published in Atmos. Chem. Phys. Discuss.: 15 November 2011

Revised: 17 April 2012 – Accepted: 17 April 2012 – Published: 3 May 2012

**Abstract.** This study evaluates the significance of glyoxal acting as an intermediate species leading to secondary organic aerosol (SOA) formation from aromatic hydrocarbon photooxidation under humid conditions. Rapid SOA formation from glyoxal uptake onto aqueous  $(\text{NH}_4)_2\text{SO}_4$  seed particles is observed in agreement with previous studies; however, glyoxal did not partition significantly to SOA (with or without aqueous seed) during aromatic hydrocarbon photooxidation within an environmental chamber (RH less than 80%). Rather, glyoxal influences SOA formation by raising hydroxyl (OH) radical concentrations. Four experimental approaches supporting this conclusion are presented in this paper: (1) increased SOA formation and decreased SOA volatility in the toluene +  $\text{NO}_x$  photooxidation system with additional glyoxal was reproduced by matching OH radical concentrations through  $\text{H}_2\text{O}_2$  addition; (2) glyoxal addition to SOA seed formed from toluene +  $\text{NO}_x$  photooxidation did not increase SOA volume under dark; (3) SOA formation from toluene +  $\text{NO}_x$  photooxidation with and without deliquesced  $(\text{NH}_4)_2\text{SO}_4$  seed resulted in similar SOA growth, consistent with a minor contribution from glyoxal uptake onto deliquesced seed and organic coatings; and (4) the fraction of a  $\text{C}_4\text{H}_9^+$  fragment (observed by Aerodyne High Resolution Time-of-Flight Aerosol Mass Spectrometer, HR-ToF-AMS) in SOA from 2-tert-butylphenol (BP) oxidation was unchanged in the presence of additional glyoxal despite enhanced SOA formation. This study suggests that glyoxal uptake onto aerosol during the oxidation of aromatic hydrocarbons is more limited than previously thought.

## 1 Introduction

Aerosol contributes to climate change and adversely affects air quality (Seinfeld and Pandis, 2006; Finlayson-Pitts and Pitts, 1999). Secondary organic aerosol (SOA) is formed from oxidative processing of volatile organic compounds in the atmosphere. Previous researchers have estimated approximately 70% of organic aerosols are secondary in nature (Hallquist et al., 2009 and references therein). Traditionally, SOA formation is described solely by gas-to-particle partitioning of semi-volatile oxidation products of volatile organic compounds (VOCs) (Odum et al., 1996; Pankow, 1994). However, recent works have observed enhanced SOA formation from the oligomerization of volatile species (Kalberer et al., 2004; Tolocka et al., 2004).

Glyoxal was previously ignored as a SOA precursor due to its high vapor pressure (6 orders of magnitude too high, Volkamer et al., 2007); however, the current view is that glyoxal can contribute to SOA formation by uptake into water (cloud, fog, and wet aerosols) followed by radical and non-radical reactions to produce low volatility products (Lim et al., 2010 and references therein). The global emission of glyoxal is estimated to be  $45 \text{ Tg yr}^{-1}$  (Fu et al., 2008); globally, the major precursor of glyoxal is isoprene ( $21 \text{ Tg yr}^{-1}$ ) (Fu et al., 2008), while aromatic hydrocarbons are the main precursors in urban areas (e.g., 70~79% in Mexico City, Volkamer et al., 2007).

The liquid water content of typical cloud droplets are orders of magnitude higher than that of aerosols (Seinfeld and Pandis, 2006); therefore, early work on glyoxal SOA

formation focused on aqueous reactions in cloud and fog water (e.g., Ervens et al., 2004). However, SOA formation from glyoxal uptake onto wet aerosols has attracted increasing attention during the last few years. Volkamer et al. (2007) observed significantly lower glyoxal concentration than model predictions for Mexico City, indicating a large missing sink of glyoxal. The discrepancy was resolved by introducing glyoxal uptake onto aerosols; ~15 % of the SOA formation in Mexico City was attributed to glyoxal uptake onto aerosols (Volkamer et al., 2007). Additionally, recent laboratory studies suggest formation of SOA via oligomerization of glyoxal in aerosol aqueous phase (Volkamer et al., 2009; Corrigan et al., 2008; Kroll et al., 2005; Galloway et al., 2009, 2011; Liggio et al., 2005b).

Glyoxal uptake onto particles is observed to be strongly dependent on seed composition. Acidity is suggested to enhance glyoxal partitioning to the aqueous phase (Jang and Kamens, 2001). However, Kroll et al. (2005) did not observe the acidity effect; instead they suggested that ionic strength of the seed aerosols (“salting in”) could explain the enhanced glyoxal uptake onto aqueous ammonium sulfate seeds (by a factor of ~70 compared to uptake by water). A more recent work by Ip et al. (2009) suggested that sulfate was a more important factor than ionic strength in affecting glyoxal’s Henry’s law constant. Organic seeds are also reported to enhance glyoxal uptake (e.g., Volkamer et al. (2009): fulvic acid, humic acid sodium salt, and amino acids; Corrigan et al. (2008): amino acids and carboxylic acids). However, understanding of the composition of SOA formed from aromatic hydrocarbon oxidation is currently limited; typically only less than ~10 % of aromatic SOA composition is identified (Sato et al., 2007; Cocker et al., 2001b; Hamilton et al., 2005). Therefore, the impact of organic aerosol on glyoxal uptake is highly uncertain.

Glyoxal is a major product of aromatic hydrocarbon photooxidation (e.g., 8~24 % from toluene-NO<sub>x</sub> photooxidation, Calvert et al., 2002). Aromatic hydrocarbons comprise ~20 % of nonmethane hydrocarbons in the urban atmosphere and are considered to be one of the major precursors to urban SOA (Calvert et al., 2002). A large number of studies have investigated gas-phase photooxidation of aromatic hydrocarbons (Olariu et al., 2002; Volkamer et al., 2002; Takekawa et al., 2003; Johnson et al., 2004; Johnson et al., 2005; Coeur-Tourneur et al., 2006; e.g., Arey et al., 2009; Calvert et al., 2002 and references therein; Birdsall et al., 2010). Although multigenerational reactions have been suggested to contribute to aromatic SOA formation (Hurley et al., 2001; Ng et al., 2007; Sato et al., 2007; Nakao et al., 2011a), the extent of the contribution from second or later generation products to SOA is poorly understood. Based on previous studies on SOA formation by glyoxal uptake, glyoxal oligomerization has been inferred to be a substantial intermediate reaction in SOA formation from aromatic hydrocarbon under humid conditions (Zhou et al., 2011; Kalberer et al., 2004; Kamens et al., 2011). According to previous studies on glyoxal

uptake, glyoxal is expected to partition to aqueous phase of SOA and subsequently undergo free-radical initiated and various condensation reactions to produce low-volatility products. However, the applicability of these previous studies of relatively pure systems (wet inorganic/organic seed) to complex aromatic SOA system remains uncertain. The aim of this work is to shed light on the role of glyoxal in SOA formation from aromatic hydrocarbon oxidation – specifically as an OH radical source or an oligomer precursor.

## 2 Experimental

### 2.1 Environmental chamber

The experiments were conducted in the UC Riverside/CE-CERT environmental chamber described in detail in Carter et al. (2005). In short, this facility consists of dual 90 m<sup>3</sup> Teflon® reactors suspended by rigid frames in a temperature controlled enclosure (27±1 °C) continuously flushed with dry (a dew point below -40 °C) purified air generated by an Aadco 737 series (Cleves, Ohio) air purification system. The top frames are slowly lowered during the experiments to maintain a slight positive differential pressure (~7.5 Pa) between the reactors and the enclosure, to minimize dilution and possible contamination of the reactors. Black lights (272 bulbs, 115 W Sylvania 350BL, NO<sub>2</sub> photolysis rate 0.4 min<sup>-1</sup>) are used as the light source for all the experiments reported herein.

### 2.2 Chemicals

NO (UHP grade, Matheson) was used for NO<sub>x</sub> photooxidation experiments. The following chemicals were all purchased from Sigma-Aldrich: toluene (>99.5 %), 2-tert-butylphenol (>99 %), perfluorohexane (>99 %), H<sub>2</sub>O<sub>2</sub> (50wt % solution in water), glyoxal trimer dihydrate (>95 %), P<sub>2</sub>O<sub>5</sub> (>98 %), glyoxal water solution (40 wt %), hexanedioic acid (>99.5 %), decanedioic acid (>99), and ammonium sulfate (>99 %).

### 2.3 Gas analysis

Glyoxal was measured by a custom-built, incoherent broadband Cavity Enhanced Absorption Spectrometer (CEAS) (Washenfelder et al., 2008; Langridge et al., 2006). In CEAS, a continuous wave incoherent light is injected into a cavity, where the intensity reaches its limiting value and absorption spectra are obtained (Engeln et al., 1998). The absorption coefficient is obtained from (Fiedler et al., 2005)

$$\alpha(\lambda) = \frac{1}{d} \left( \frac{I_0(\lambda)}{I(\lambda)} - 1 \right) (1 - R(\lambda)) \quad (1)$$

where  $\alpha$  is the absorption coefficient,  $d$  is the length of the cavity,  $I_0$  is the intensity of light exiting the cavity without any absorber present,  $I$  is the light intensity of the cavity

with absorber, and  $R$  is the reflectivity of the mirrors. In CEAS, the transmitted light intensity through the optical cavity of two high reflectivity mirrors provides sensitive measurements of trace species with a long effective optical path (Engeln et al., 1998; Paul, 2001; Fiedler, 2003; Langridge et al., 2006; Washenfelder, 2008). CEAS allows for simultaneous analysis of multiple absorbers in the same spectral region (e.g., both  $\text{NO}_2$  and glyoxal in the 440–460 nm region).

In this work, the CEAS system for the glyoxal measurements was based on the previous work by Langridge et al. (2006) and Washenfelder et al. (2008). The major components of the CEAS system include a glass cell housing the optical cavity (65 cm long, 2.54 cm diameter with 1/16 inch wall thickness), two high reflectivity ( $R = 0.9998$ ) mirrors (Los Gatos), a light emitting diode (LED) (Luxeon) light source, a monochromator and a charge-coupled device (CCD) light detector (Andor). The light from the LED was focused and coupled into the optical cavity; the output light from the cavity was dispersed by the monochromator and collected by the CCD detector. Gas flow rate through the CEAS was 1 LPM, while the pressure inside the optical cavity ranged from 714–720 Torr (0.939–0.947 atm). The CCD collected the transmission spectra from the cavity using an exposure time of 0.5 second, with 112 samples accumulated during an overall sampling time of 1 min. The 0.5 second exposure time was chosen to prevent saturation of the signal at the peak LED emission spectrum at the maximum operating power of 200 mW for this CEAS system. The background signal, under the same acquisition conditions, was collected with the LED off and the background spectra was subtracted from the transmission spectra from the cavity.

The glyoxal number density was calculated from

$$\alpha(\lambda) = b_0 + b_1 \cdot \lambda + b_2 \cdot \lambda^2 + b_3 \cdot \lambda^3 + \sigma_{\text{NO}_2}(\lambda) \cdot n_{\text{NO}_2} + \sigma_{\text{gly}}(\lambda) \cdot n_{\text{gly}} \quad (2)$$

where  $\lambda$  is the wavelength,  $\sigma_{\text{gly}}$  is glyoxal absorption cross-section,  $n_{\text{gly}}$  is the glyoxal number density,  $\alpha(\lambda)$  is the measured absorption coefficient for a given  $\lambda$ , the polynomial terms of the equation account for light extinction by background molecules (e.g.,  $\text{N}_2$  and  $\text{O}_2$ ), and  $\sigma_{\text{NO}_2}$  and  $n_{\text{NO}_2}$  account for light absorption by  $\text{NO}_2$ . Wavelength-dependent absorption cross-sections ( $\sigma(\lambda)$ ) were obtained from literature and data evaluation web sites (e.g., IUPAC, 2006; NASA, 2006; Volkamer et al., 2005). The glyoxal number densities were extracted using the spectra between 446.5 and 450.0 nm.

The Agilent 6890 Gas Chromatograph – Flame Ionization Detector was used to measure concentrations of parent hydrocarbons (toluene and 2-tert-butylphenol) and an inert tracer (perfluorohexane). A GS-Alumina column (30 m × 0.53 mm) and a DB-5 column (30 m × 0.53 mm) were used for perfluorohexane and toluene analysis, respectively. 2-tert-butylphenol was collected on a sorbent tube packed with Tenax-TA/Carbopack/Carbosive (CDS Analytical, Inc, MX062171) and was thermally desorbed at 290 ° (CDS Analytical, Inc, ACEM9305) onto a Restek® Rtx-35 Amine

(30 m × 0.53 mm ID, 1.00 micron) column. Toluene measurements were calibrated using a dilute gas cylinder (SCOTT-MARIN, Inc); perfluorohexane was calibrated by introducing a known amount of the liquid into the reactor; and 2-tert-butylphenol was calibrated by impregnation of the glass tube and subsequent thermal desorption.

## 2.4 Particle analysis

Particle size distribution between 27 nm and 686 nm was monitored by a custom built Scanning Mobility Particle Sizer (SMPS) similar to that described by Cocker et al. (2001a). The chemical evolution of organic particulate matter was observed by a high-resolution time-of-flight aerosol mass spectrometer (HR-ToF-AMS) (DeCarlo et al., 2006; Jayne et al., 2000). The HR-ToF-AMS operation was alternated between the high resolution W-mode and high sensitivity V-mode. The high resolution capability allowed determination of molecular formula of ion fragments of SOA (e.g.,  $\text{C}_4\text{H}_9^+$ ). SQUIRREL v1.49 and PIKA v1.08 were used for data analysis. The default fragmentation table was used without modification. Particle volatility was monitored with a volatility tandem differential mobility analyzer (VTDMA) (Nakao et al., 2011b; Qi et al., 2010b; Rader and McMurry, 1986), in which monodisperse particles of mobility diameter  $D_{mi}$  were selected by the 1st differential mobility analyzer (DMA) followed by transport through a Dekati thermodenuder (TD, residence time: ~17 s, typically at 100 °). The particle size after the TD ( $D_{mf}$ ) was then measured by fitting a log-normal size distribution curve acquired by the 2nd DMA. Volume fraction remaining (VFR) was calculated by taking a (cubed) ratio of particle mobility diameter after the TD ( $D_{mf}$ ) to initial particle size ( $D_{mi}$ ), i.e.,  $\text{VFR} = (D_{mf}/D_{mi})^3$ .  $D_{mi}$  was adjusted during the experiment according to mode diameters of particle size distribution within the environmental chamber to maximize the signal-to-noise ratio (typically  $D_{mi} = 50\sim 150\text{nm}$ ). Particle hygroscopicity as a function of RH was monitored with a hygroscopicity TDMA (HTDMA) (Cocker et al., 2001a; Qi et al., 2010a; Warren et al., 2009). Volume based hygroscopic growth factor was monitored in a similar way as VFR, i.e., by taking a cubed ratio of particle mobility diameter after a humidification column to initially selected particle size.

## 2.5 Thermodenuder characterization

As a basis to evaluate the VFR in terms of vapor pressure, thermodenuder characterization was performed by measuring the VFR of select compounds with known vapor pressure ( $D_{mi} = 150\text{nm}$ ). The vaporization profile was previously evaluated based on the temperature at which 50 % of the mass evaporates ( $T_{50}$ ) (Faulhaber et al., 2009). The vaporization profiles for hexanedioic acid and decanedioic acid acquired in this study agreed reasonably with Fualhaber et al. (2009) ( $T_{50}$  agreed within 2 °), consistent with the similar residence

**Table 1.** Experimental test matrix.

Run ID	Run type	Aromatic <sub>i</sub> <sup>a</sup> (ppb)	Aromatic <sub>f</sub> <sup>b</sup> (ppb)	ΔAromatic (μg m <sup>-3</sup> )	M <sub>org+water</sub> <sup>c</sup> (μm <sup>3</sup> cm <sup>-3</sup> )	NO <sup>a</sup> (ppb)	H <sub>2</sub> O <sub>2</sub> <sup>d</sup> (ppm)	Glyoxal <sup>a</sup> (ppb)	RH (%)	Seed volume <sup>a</sup> (μm <sup>3</sup> cm <sup>-3</sup> )	LWC (% mass)
1368A	glyoxal + AS <sup>e</sup>	–	–	–	12.0	–	–	46	74	101.0	51 <sup>f</sup>
1499B	toluene + NO <sub>x</sub>	70.5	9.4	230	25.5	46.3	–	–	< 0.1	–	0
1503A	toluene + NO <sub>x</sub>	100.7	16.8	316	57.1	41.5	–	–	40	–	1 <sup>g</sup>
1497A	toluene + NO <sub>x</sub>	94.9	39.6	208	65.9	47.1	–	–	65	–	6 <sup>g</sup>
1497B	toluene + NO <sub>x</sub>	94.8	47.4	179	65.9	22.5	–	–	65	–	6 <sup>g</sup>
1498A	toluene + NO <sub>x</sub>	100.0	30.4	262	65.0	40.2	–	–	75	–	10 <sup>g</sup>
1500B	toluene + NO <sub>x</sub>	104.2	30.4	278	77.7	45.3	–	–	70	–	8 <sup>g</sup>
1501A	toluene + NO <sub>x</sub> + glyoxal	101.7	20.5	306	107.0	43.2	–	80	75	–	10 <sup>g</sup>
1501B	toluene + NO <sub>x</sub> + H <sub>2</sub> O <sub>2</sub>	100.9	22.8	294	98.2	43.2	0.3	–	75	–	10 <sup>g</sup>
1509A	toluene + NO <sub>x</sub> + H <sub>2</sub> O <sub>2</sub>	98.3	26.4	271	89.0	42.6	0.3	–	72	–	9 <sup>g</sup>
1510A	toluene + NO <sub>x</sub> + AS	102.0	25.2	289	82.4	42.8	–	–	79	56.9	56 <sup>f</sup>
1510B	toluene + NO <sub>x</sub> + AS	102.3	24.1	295	104.2	42.8	–	–	79	83.1	56 <sup>f</sup>
1511A	toluene + NO <sub>x</sub> + AS	95.6	29.0	251	71.2	40.5	–	–	78	61.5	55 <sup>f</sup>
1511B	toluene + NO <sub>x</sub> + AS	95.6	27.9	255	94.3	40.7	–	–	78	59.1	55 <sup>f</sup>
1489A	2t-BP + H <sub>2</sub> O <sub>2</sub>	124.0	26.2	601	52.8	–	0.3	720 <sup>d</sup>	51	–	1 <sup>g</sup>

<sup>a</sup>: Initial concentration <sup>b</sup>: Final concentration <sup>c</sup>: Wall-loss corrected organic (+ water) volume measured by SMPS <sup>d</sup>: Calculated using injected amount <sup>e</sup>: AS: ammonium sulfate <sup>f</sup>: Calculated using ISORROPIA Nenes et al. (1998) <sup>g</sup>: Calculated using M<sub>org+water</sub> and a humidogram for toluene SOA

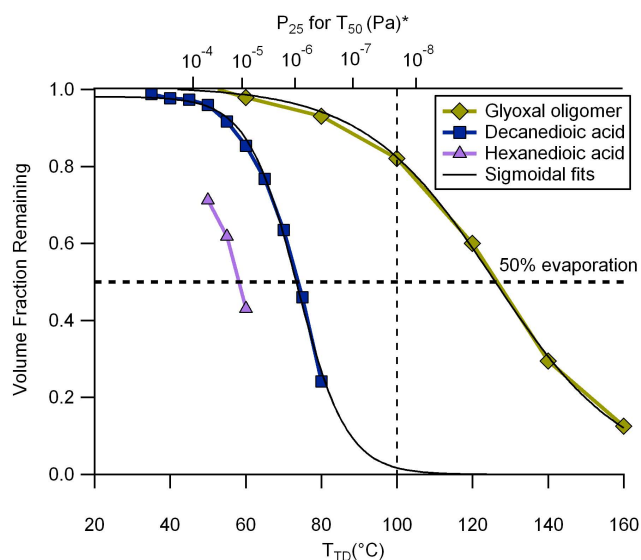


**Fig. 1.** Thermograms of hexanedioic acid, decanedioic acid, and glyoxal oligomer (produced from evaporating droplets of glyoxal/water solution) where  $T_{TD}$  is the set temperature of the thermodenuder and  $P_{25}$  is the vapor pressure of a compound at 25 °C (\*calibration taken from Faulhaber et al., 2009).

times of the thermodenuders (This study: ~17 sec, Fualhaber et al. (2009): ~15 s). Therefore we applied their vapor pressure calibration for approximate evaluation of SOA vapor pressure in this study (Fig. 1).

The volatility of glyoxal oligomer was evaluated by generating glyoxal oligomer from evaporating droplets (De Haan et al., 2009a). Glyoxal solution in water (40 wt %) was aerosolized by an atomizer into a 0.6 m<sup>3</sup> Teflon chamber. As water evaporated from the droplet, dihydrated glyoxal lost water to form more reactive monohydrated glyoxal, which

then self-oligomerized to form low-volatility compounds (De Haan et al., 2009a). The vaporization profile suggested that the vapor pressure of dried glyoxal oligomer was much lower than 10<sup>-8</sup> Pa, where reliable vapor pressure measurement is not possible. Since dehydration is the key process of this oligomer formation, vapor pressure of oligomers could be higher if water is retained in particles. Vapor pressure of organosulfates (Surrat et al., 2007; Galloway et al., 2009) or nitrogen-containing species (Galloway et al., 2009; De Haan et al., 2009b) remains uncertain.

## 2.6 Chamber experiments

The experimental test matrix is summarized in Table 1. A known volume of high purity liquid hydrocarbon was injected through a heated glass injection manifold system and flushed into the chamber with pure N<sub>2</sub>. Injection of 2-tert-butylphenol and H<sub>2</sub>O<sub>2</sub> was performed in the same way as described in Nakao et al. (2011a). Since phenolic compounds are less volatile than hydrocarbons typically used for chamber experiments, injections into the chambers were carefully performed using a heated oven (50~80 °) through a heated transfer line maintained at a temperature higher than the oven. The glass manifold inside the oven was packed with glass wool to increase the mass transfer surface area. H<sub>2</sub>O<sub>2</sub> was used as an additional OH radical source to test the role of glyoxal. H<sub>2</sub>O<sub>2</sub> 50wt % solution was injected through the same oven system. Particle-free water vapor was injected using a two-unit system (Warren et al., 2009). Unit one contained Milli-Q water (Millipore, 18.2MΩ) with submerged heaters to maintain a desired water temperature, which determined the water vapor concentration in the air stream, while unit two contained a 1 μm filter. Purified air was bubbled through the water and then passed through the filter before entering the reactors. Humidity in the reactor

was monitored by a humidity and temperature transmitter (VAISALA HMT334). Deliquesced  $(\text{NH}_4)_2\text{SO}_4$  seed particles were generated by aerosolizing dilute  $(\text{NH}_4)_2\text{SO}_4$  solution in Milli-Q water by a custom-built atomizer, followed by Kr-85 neutralizer (TSI, model 3077) without drying. Seed particles were confirmed to be deliquesced by using VT-DMA; evaporation of water from particles was observed by loss of volume after passing particles through a thermodeuder. Particle wall-loss correction was performed by using exponential decay rates of particle numbers (Carter et al., 2005).

### 3 Results and discussion

#### 3.1 Glyoxal uptake onto deliquesced $(\text{NH}_4)_2\text{SO}_4$

Significant SOA formation by glyoxal uptake onto deliquesced  $(\text{NH}_4)_2\text{SO}_4$  was observed under dark conditions (Fig. 2). Wet ammonium sulfate seed particles were injected into the chamber ( $\text{RH} = 74\%$ ) and allowed to equilibrate, followed by glyoxal injection. Immediately following the glyoxal injection, the organic/sulfate ratio measured by the AMS increased due to glyoxal uptake, reaching a maximum value of  $\sim 0.4$  around 6 h after glyoxal injection. After reaching maximum organic/sulfate ratio, the environmental chamber was diluted; organic/sulfate ratio decreased due to evaporation of glyoxal oligomers, suggesting glyoxal oligomerization is reversible, as also observed by Galloway et al. (2009). The slower decrease of glyoxal concentration than tracer concentration is consistent with the large glyoxal-reservoir effect of chamber surface (Loza et al., 2010). In a separate experiment (not shown), no increase in organic/sulfate ratio is observed for a similar experiment conducted under dry conditions ( $\text{RH} < 0.1\%$ ), confirming the critical role of aqueous phase of  $(\text{NH}_4)_2\text{SO}_4$  seed particles in glyoxal oligomerization (Galloway et al., 2009; Liggio et al., 2005b; Kroll et al., 2005).

#### 3.2 Evaluation of glyoxal uptake onto toluene SOA

Glyoxal uptake during SOA formation from toluene photooxidation was investigated under humid conditions ( $\text{RH} 40\text{--}80\%$ ). Previous studies observed oligomers in aromatic SOA formed within this  $\text{RH}$  range (e.g.,  $\text{RH} 40\text{--}50\%$ , Kalberer et al., 2004; Kalberer et al., 2006); heterogeneous reactions or particle-phase reaction of dicarbonyls, in particular glyoxal and methylglyoxal, were proposed to be important reaction mechanisms (Kalberer et al., 2004; Healy et al., 2008). However, the significance of glyoxal uptake in the aromatic SOA system has not been evaluated directly; this section evaluates the significance of glyoxal uptake onto toluene SOA during irradiated and dark conditions.

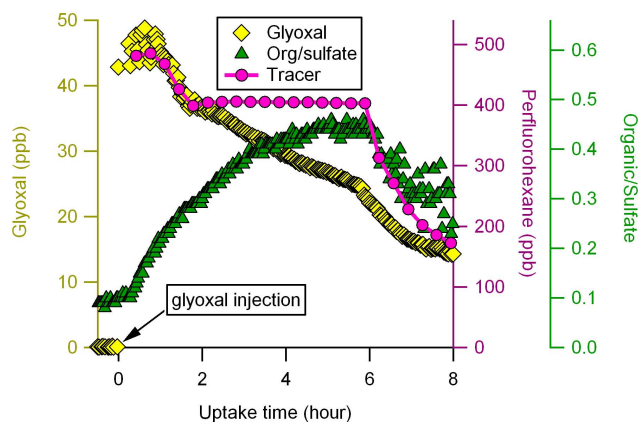


**Fig. 2.** Typical time traces of glyoxal, organic/sulfate ratio, and tracer (perfluorohexane) during toluene- $\text{NO}_x$  photooxidation (Run 1368A). Immediately after glyoxal injection, organic/sulfate ratio increased. Upon dilution at 6 h after injection, organic/sulfate ratio decreased due to evaporation of organics, consistent with Galloway et al. (2009).

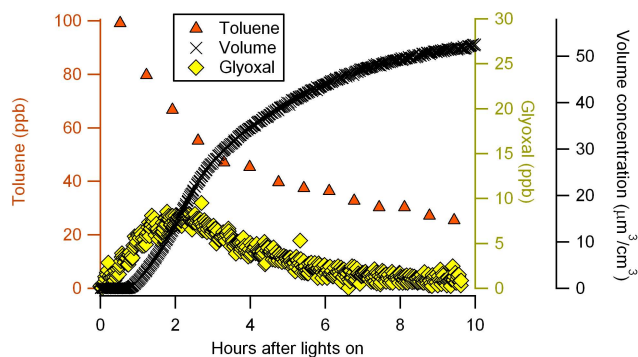


**Fig. 3.** The time traces of toluene, particle volume concentration, and glyoxal concentration during toluene- $\text{NO}_x$  photooxidation. (Run 1503A). Typically glyoxal concentration was below 10 ppb.

#### 3.2.1 Irradiated conditions

A representative toluene photooxidation experiment including toluene decay, SOA formation, and glyoxal formation is shown in Fig. 3. Typically, glyoxal concentration remained below 10 ppb. The impact of glyoxal on SOA formation for the toluene photooxidation system was evaluated by injecting 80 ppb additional glyoxal into the system (Fig. 4). The addition of 80 ppb glyoxal in the toluene +  $\text{NO}_x$  oxidation system resulted in faster toluene decay and higher SOA formation (green trace in Fig. 4). Since toluene predominantly reacts with OH radicals (reactions of toluene with  $\text{O}_3$  or  $\text{NO}_3$  are slow, Calvert et al., 2002), the faster toluene decay indicates that OH radical concentration was enhanced by glyoxal photolysis. OH radical also influences aqueous chemistry (Volkamer et al., 2009) in addition to gas-phase chemistry (Calvert et al., 2002). To elucidate the role of increased OH

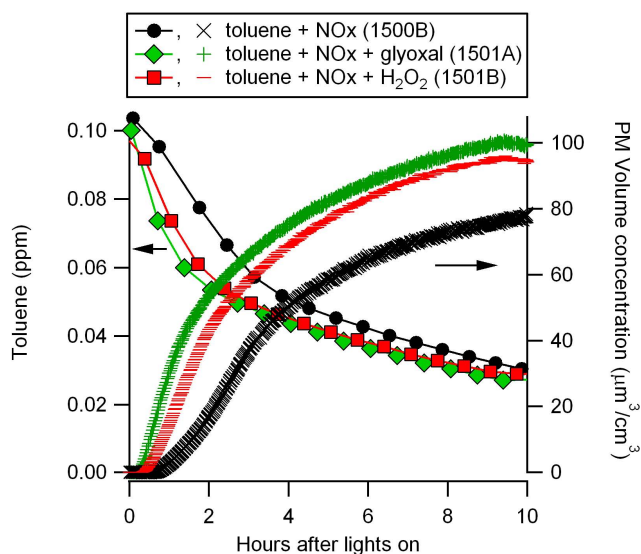


**Fig. 4.** Evaluation of glyoxal impact as a radical source. Addition of glyoxal (green trace) and  $\text{H}_2\text{O}_2$  (red trace) resulted in nearly identical toluene decay and SOA formation, indicating that glyoxal acted as a radical source, instead of an oligomer precursor.

radical versus glyoxal uptake, another toluene- $\text{NO}_x$  photooxidation experiment with elevated  $\text{H}_2\text{O}_2$  concentration (added to match OH levels in the additional glyoxal experiment) was performed (red trace in Fig. 4). Addition of  $\text{H}_2\text{O}_2$  resulted in practically identical toluene decays between the  $\text{H}_2\text{O}_2$  and glyoxal experiments. The similar toluene decay rates in these additional glyoxal/ $\text{H}_2\text{O}_2$  experiments indicate successful matching of OH levels. For these two experiments, SOA formation was nearly identical, suggesting that the major impact of glyoxal was enhanced OH level, with insignificant contributions of glyoxal to SOA formation by direct uptake. In addition to particle volume, particle volatility was monitored to evaluate glyoxal uptake onto SOA during irradiation. The evolution of VFR at  $100^\circ$  of toluene SOA was monitored by VTDMA (Fig. 5). The VFR of toluene SOA rapidly increased and plateaued after  $\sim 6$  h. The addition of glyoxal to the photooxidation system resulted in increased VFR. One might interpret this as contribution of glyoxal oligomer. However, the addition of  $\text{H}_2\text{O}_2$  as a radical source resulted in nearly an identical profile, again suggesting that the role of glyoxal in toluene SOA formation (under irradiation) in this study was as a radical source, not an oligomer precursor.

### 3.2.2 Dark conditions

The absence of glyoxal uptake onto the toluene SOA was further investigated by the addition of glyoxal after SOA formation in the dark as a “SOA seed” experiment (Fig. 6). Blacklights were turned off after  $\sim 9$  h of irradiation and nearly 100 ppb glyoxal was injected; no significant increase

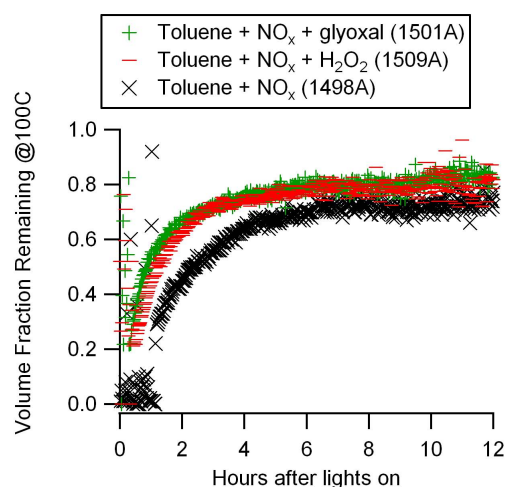


**Fig. 5.** The time traces of particle volume fraction remaining at  $100^\circ$ . Addition of both glyoxal and  $\text{H}_2\text{O}_2$  resulted in faster reaction and slightly less volatile particles, indicating that glyoxal acted as a radical source.

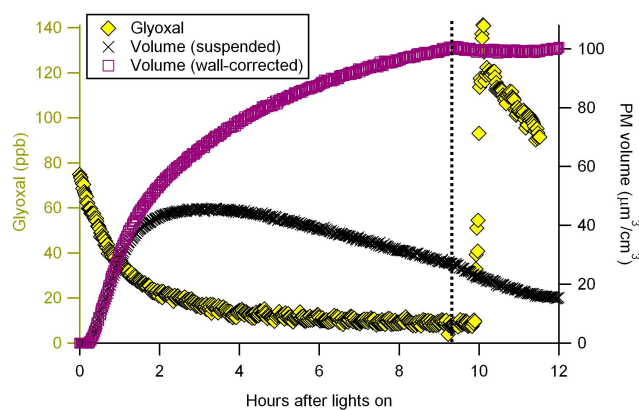


**Fig. 6.** The time traces of glyoxal and particle volume concentration (suspended and wall-loss corrected) (Run 1501A). The dashed line indicates the time blacklights were turned off. Addition of glyoxal ( $\sim 100$  ppb) at 10 h into SOA seed system did not form significant SOA.

in particle volume concentration was observed. The absence of glyoxal uptake onto SOA seed is in contrast with the aforementioned significant glyoxal uptake onto deliquesced  $(\text{NH}_4)_2\text{SO}_4$ ; the difference highlights the importance of liquid water content (LWC) and/or electrolytes in glyoxal uptake as discussed below.

### 3.2.3 Impact of LWC and electrolytes

Previous studies proposed LWC as a major contributor to SOA formation via aqueous reactions (Volkamer et al., 2009; Kamens et al., 2011; Zhou et al., 2011). LWC for toluene SOA at a given RH was estimated using a humidogram acquired from a dry toluene +  $\text{NO}_x$  experiment (Fig. 7) and

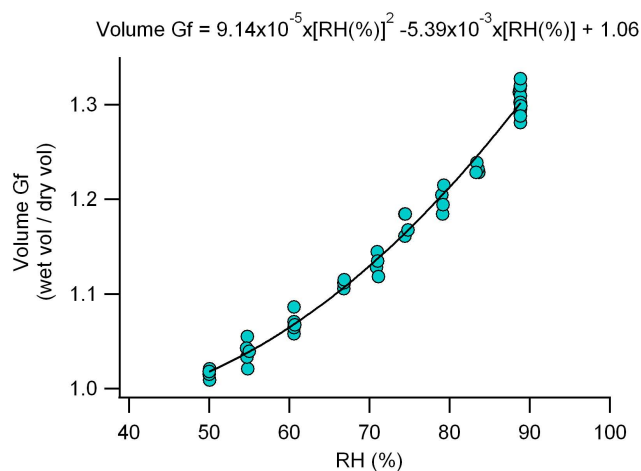


**Fig. 7.** Humidogram of SOA formed by the photooxidation of toluene + NO<sub>x</sub> under a dry condition (Run 1499B).

shown in Table 1 (a volume ratio taken from the humidogram is converted into a mass fraction assuming SOA density 1.4 g cm<sup>-3</sup>). LWC for deliquesced (NH<sub>4</sub>)<sub>2</sub>SO<sub>4</sub> was estimated using ISORROPIA (Nenes et al., 1998). The absence of significant glyoxal uptake onto toluene SOA can be interpreted as a result of smaller LWC of SOA than that of (NH<sub>4</sub>)<sub>2</sub>SO<sub>4</sub> (Table 1), which is in agreement with the growing belief that liquid water is needed for glyoxal uptake (e.g., Volkamer et al., 2009; Kamens et al., 2011). In order for glyoxal uptake to significantly occur during the irradiated conditions in this study, higher LWC, rather than higher RH, might be required (Kamens et al., 2011). In addition, the composition of the aqueous phase matters to glyoxal uptake; previous studies reported enhanced partitioning of glyoxal into water containing sulfate ion (Ip et al., 2009) and catalytic effect of ammonium ion on glyoxal oligomerization (Nozière et al., 2008). Kroll et al. (2005) observed far higher (by a factor of ~70) glyoxal uptake onto deliquesced (NH<sub>4</sub>)<sub>2</sub>SO<sub>4</sub> than by pure water. The absence of glyoxal uptake onto toluene SOA shown in Fig. 6 suggests that aqueous phase of toluene SOA may not be preferable for glyoxal uptake.

### 3.3 Effect of deliquesced (NH<sub>4</sub>)<sub>2</sub>SO<sub>4</sub> seed on toluene SOA formation

Deliquesced (NH<sub>4</sub>)<sub>2</sub>SO<sub>4</sub> was confirmed to rapidly form SOA in the presence of glyoxal (Fig. 2). If glyoxal uptake onto deliquesced (NH<sub>4</sub>)<sub>2</sub>SO<sub>4</sub> is a major mechanism of toluene SOA formation, the presence of deliquesced (NH<sub>4</sub>)<sub>2</sub>SO<sub>4</sub> seed particles is expected to enhance the toluene SOA formation significantly. SOA growth curves (SOA formation vs. hydrocarbon consumption) for non-seeded (nucleation) experiments and deliquesced (NH<sub>4</sub>)<sub>2</sub>SO<sub>4</sub> seeded experiments are shown in Fig. 8. No significant difference in those two systems was observed, suggesting that non-glyoxal routes dominated the aromatic SOA formation pathways.

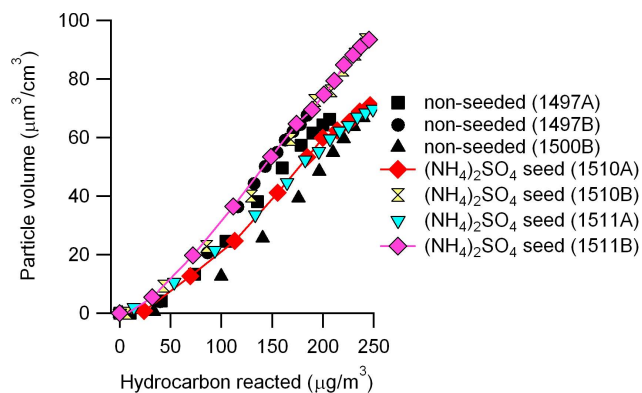


**Fig. 8.** SOA growth curves (particle volume vs. toluene reacted) of non-seeded experiments and deliquesced ammonium sulfate seed experiments. No significant difference in particle growth between those two systems was observed, indicating that contribution from glyoxal uptake onto deliquesced ammonium sulfate was minor in this system.

Although the presence of deliquesced (NH<sub>4</sub>)<sub>2</sub>SO<sub>4</sub> seed particles results in higher LWC, SOA formation from toluene photooxidation is not enhanced (Fig. 8). This is in contrast with the aforementioned impact of LWC and electrolytes on glyoxal uptake (Sect. 3.2.3). A possible explanation is that the high concentration of SOA overwhelmed the pre-existing seed particles thereby reducing the apparent seed effects; assuming the same extent of glyoxal uptake onto ammonium sulfate occurred as in the glyoxal + seed experiment, glyoxal SOA would comprise only a minor mass fraction of toluene SOA since the seed mass fraction dropped to approximately 10% in six hours (not shown) and glyoxal oligomer/sulfate ratio would be approximately 0.4 (Fig. 2). Applying the results of dark glyoxal uptake to irradiated conditions is uncertain due to the possibility of fast photochemical uptake of glyoxal (Volkamer et al., 2009); however, Galloway et al. (2011) did not observe fast photochemical uptake, and hence the significance of the fast photochemical uptake is highly uncertain. Another possible explanation for the absence of seed effects is core-shell morphology of SOA-deliquesced (NH<sub>4</sub>)<sub>2</sub>SO<sub>4</sub> particles (e.g., Smith et al., 2011; Bertram et al., 2011; Anttila et al., 2006); an organic coating around deliquesced (NH<sub>4</sub>)<sub>2</sub>SO<sub>4</sub> core may slow down the uptake of glyoxal induced by LWC and the electrolytes, resulting in reduction of the seed effects.

### 3.4 Evaluation of glyoxal uptake onto 2-tert-butylphenol SOA

The absence of significant SOA formation from glyoxal uptake onto toluene SOA is further probed by using 2-tert-butylphenol as a parent aromatic compound. When SOA formed from 2-tert-butylphenol was introduced into the HR-ToF-AMS, significant signals of the C<sub>4</sub>H<sub>9</sub><sup>+</sup> fragment from the tert-butyl substituent were observed. Since glyoxal

oligomerization can not produce  $C_4H_9^+$ ,  $C_4H_9^+$  can be used as a tracer for the SOA from 2-tert-butylphenol oxidation. The phenolic functionality (-OH) was used to enhance the reactivity of aromatic ring (e.g., *o*-cresol is seven times more reactive than toluene, Calvert et al., 2002) and to minimize the reaction of the tert-butyl substituent. Although the steric hindrance by the tert-butyl group remains uncertain, adequately similar aromatic oxidation reaction is expected for the purpose of evaluating glyoxal uptake. The result of 2-tert-butylphenol oxidation is shown in Fig. 9. Glyoxal addition to this system during photooxidation (at 10 h after lights on) resulted in enhanced SOA formation; however the fraction of  $C_4H_9^+$  in the total organics ( $f_{C_4H_9}$ ) did not change significantly indicating that aerosol formation from products not containing  $C_4H_9^+$  fragments (glyoxal and its products) was not enhanced after glyoxal injection and oxidation. This further confirms that glyoxal's influence on SOA formation in the aromatic photooxidation systems under humid conditions (RH 51 % for this experiment) is limited to increasing SOA formation by increasing gas-phase OH radical concentrations and not by reactive uptake of glyoxal into the SOA.

### 3.5 Comparison with previous studies

Consistencies and differences with previous studies are summarized in this section. Under dark conditions, this study observed significant SOA formation from glyoxal uptake onto deliquesced  $(NH_4)_2SO_4$  seed, consistent with previous studies (e.g., Galloway et al., 2009; Kroll et al., 2005; Liggio et al., 2005a; Volkamer et al., 2009). However, glyoxal uptake onto SOA seed was not observed under dark/humid conditions (section 3.2.2); this is in agreement with the importance of LWC and electrolytes (Kamens et al., 2011; Volkamer et al., 2009; Ip et al., 2009).

Recent studies by Zhou et al. (2011) and Kamens et al. (2011) observed that particle water concentration was highly related to SOA formation from aromatic hydrocarbons (toluene and xylenes), which was largely explained by oligomerization of glyoxal (to a lesser extent, methylglyoxal) in aqueous phase. Since this study also observed higher SOA formation for high RH and LWC experiments (e.g., Run 1499B vs., 1497A, Table 1), our results are partly in agreement with their study. However, our direct measurement of glyoxal by CEAS, along with experiments using synthesized glyoxal, strongly indicates glyoxal uptake was insignificant during aromatic SOA formation, at least in our experimental conditions (e.g., LWC, SOA loadings).

One of the differences between this study and their study is particle concentration ranges: Zhou et al. (2011) and Kamens et al. (2011) – from  $\sim 1$  to  $\sim 30 \mu g m^{-3}$ ; this study – from  $\sim 30 \mu g m^{-3}$  to over  $100 \mu g m^{-3}$ . Since glyoxal uptake is not driven by partitioning to organics but by dissolution into water (Volkamer et al., 2009), glyoxal uptake might preferentially occur in their low organic aerosol/high RH experiments (over 90 % for some experiments). Also, the higher

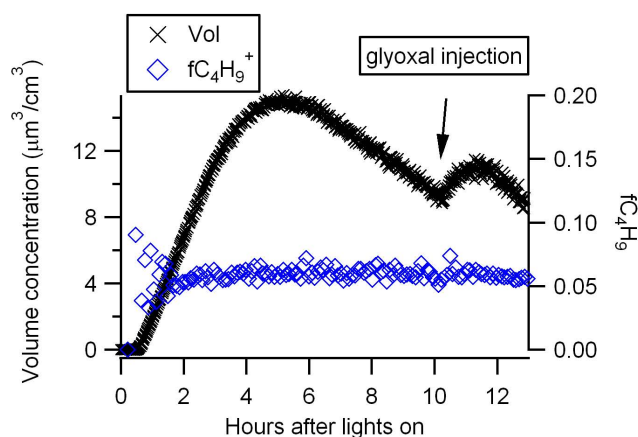


**Fig. 9.** The time traces of particle volume formed from 2-tert-butylphenol photooxidation and  $C_4H_9^+$  fragment in particles (Run 1489A). Particle volume increased immediately after glyoxal injection while the fraction of  $C_4H_9^+$  in organics was unaffected, indicating the increase of particle volume was due to enhanced reaction of 2-tert-butylphenol, as opposed to glyoxal uptake.

SOA formation in the higher LWC experiments (observed in both their study and this study) could be explained by aqueous reactions of water-soluble products other than glyoxal, such as phenolic compounds (Sun et al., 2010). Different experimental conditions such as light sources (natural vs. blacklights) or background composition may also contribute to the different observations.

Applicability of this study on aromatics to other compounds, such as biogenic compounds, remains uncertain. However, assuming LWC is the key parameter in glyoxal uptake (Kamens et al., 2011), similar results are expected for biogenic SOA since hygroscopic growth factors of biogenic SOA were often observed to be approximately same as (or slightly less than) those of aromatic SOA (Jimenez et al. (2009) –  $\alpha$ -pinene, isoprene, and trimethylbenzene; Cocker et al. (2001b) –  $\alpha$ -pinene, *m*-xylene, and 1,3,5-trimethylbenzene; Qi et al. (2010a) –  $\alpha$ -pinene and *m*-xylene; Prenni et al. (2007) –  $\alpha$ -pinene,  $\beta$ -pinene,  $\Delta^3$ -carene, and toluene). Thus, further evaluation of glyoxal uptake onto biogenic SOA would be beneficial.

## 4 Conclusion

The significance of glyoxal uptake in SOA formation from aromatic hydrocarbon photooxidation was evaluated for the first time. Glyoxal uptake onto deliquesced  $(NH_4)_2SO_4$  seed resulted in rapid SOA formation as shown in previous studies; however, no significant glyoxal uptake onto SOA formed from aromatic hydrocarbon oxidation was observed. Instead of contributing to SOA formation by reactive uptake, glyoxal acted as an OH radical source following photolysis. This study suggests that the uptake and/or subsequent reaction of



glyoxal in aqueous phase of aerosol to form low-volatility compounds contributes to only minor fraction of aromatic SOA in an environmental chamber (RH less than 80 %). This study highlights the need for evaluating glyoxal uptake onto SOA seed. This study does not preclude glyoxal uptake onto aromatic SOA at RH above 80 % (or higher LWC), uptake onto non-aromatic SOA, or glyoxal cloud processing.

*Acknowledgements.* We gratefully acknowledge funding support from University of California Transportation Center, W. M. Keck Foundation, National Science Foundation (ATM-0449778, ATM-0901282, and CHE-0848643), California Air Resources Board, and University of California, Riverside, Department of Chemical and Environmental Engineering. We also acknowledge Kurt Bumiller and Charles Bufalino for experimental setup, Melissa Galloway, Arthur Chan, and Sarah Bates for helping glyoxal synthesis, Gookyoung Heo and William P. L. Carter for helpful discussions. Any opinions, findings, and conclusions or recommendations expressed in this material are those of the authors and do not necessarily reflect the views of the National Science Foundation.

Edited by: F. Keutsch

## References

- Anttila, T., Kiendler-Scharr, A., Tillmann, R., and Mentel, T. F.: On the reactive uptake of gaseous compounds by organic-coated aqueous aerosols: theoretical analysis and application to the heterogeneous hydrolysis of  $\text{N}_2\text{O}_5$ , *J. Phys. Chem. A*, 110, 10435–10443, 2006.
- Arey, J., Obermeyer, G., Aschmann, S. M., Chattopadhyay, S., Cusick, R. D., and Atkinson, R.: Dicarbonyl products of the OH radical-initiated reaction of a series of aromatics hydrocarbons, *Environ. Sci. Technol.*, 43, 683–689, 2009.
- Bertram, A. K., Martin, S. T., Hanna, S. J., Smith, M. L., Bodsworth, A., Chen, Q., Kuwata, M., Liu, A., You, Y., and Zorn, S. R.: Predicting the relative humidities of liquid-liquid phase separation, efflorescence, and deliquescence of mixed particles of ammonium sulfate, organic material, and water using the organic-to-sulfate mass ratio of the particle and the oxygen-to-carbon elemental ratio of the organic component, *Atmos. Chem. Phys.*, 11, 10995–11006, 10, <http://www.atmos-chem-phys.net/11/10995/10/.5194/acp-11-10995-2011>, 2011.
- Birdsall, A. W., Andreoni, J. F., and Elrod, M. J.: Investigation of the role of bicyclic peroxy radicals in the oxidation mechanism of toluene, *J. Phys. Chem.*, 114, 10655–10663, 2010.
- Calvert, J. G., Atkinson, R., Becker, K. H., Kamens, R. M., Seinfeld, J. H., Wallington, T. J., and Yarwood, G.: *The mechanism of atmospheric oxidation of aromatics hydrocarbons*, Oxford University Press, New York, USA, 2002.
- Carter, W. P. L., Cocker, D. R., Fitz, D. R., Malkina, I. L., Bumiller, K., Sauer, C. G., Pisano, J. T., Bufalino, C., and Song, C.: A new environmental chamber for evaluation of gas-phase chemical mechanisms and secondary aerosol formation, *Atmos. Environ.*, 39, 7768–7788, 2005.
- Cocker, D. R., Flagan, R. C., and Seinfeld, J. H.: State-of the art chamber facility for studying atmospheric aerosol chemistry, *Environ. Sci. Technol.*, 35, 2594–2601, 2001a.
- Cocker, D. R., Mader, B. T., Kalberer, M., Flagan, R. C., and Seinfeld, J. H.: The effect of water on gas-particle partitioning of secondary organic aerosol: 2. m-xylene and 1,3,5-trimethylbenzene photooxidation systems, *Atmos. Environ.*, 35, 6073–6085, 2001b.
- Coeur-Tourneur, C., Henry, F., Janquin, M.-A., and Brutier, L.: Gas-phase reaction of hydroxyl radicals with m-, o- and p-cresol, *Int. J. Chem. Kin.*, 38, 553–562, 2006.
- Corrigan, A. L., Hanley, S. W., and De Haan, D. O.: Uptake of Glyoxal by Organic and Inorganic Aerosol, *Environ. Sci. Technol.*, 42, 4428–4433, doi:10.1021/es7032394, 2008.
- De Haan, D. O., Corrigan, A. L., Tolbert, M. A., Jimenez, J. L., Wood, S. E., and Turley, J. J.: Secondary Organic Aerosol Formation by Self-Reactions of Methylglyoxal and Glyoxal in Evaporating Droplets, *Environ. Sci. Technol.*, 43, 8184–8190, 10.1021/es902152t, 2009a.
- De Haan, D. O., Tolbert, M. A., and Jimenez, J. L.: Atmospheric condensed-phase reactions of glyoxal with methylamine, *Geophys. Res. Lett.*, 36, L11819, doi:10.1029/2009gl037441, 2009b.
- DeCarlo, P. F., Kimmel, J. R., Trimborn, A. M., Northway, M., Jayne, J. T., Aiken, A. C., Gonin, M., Fuhrer, K., Horvath, T., Docherty, K., Worsnop, D. R., and Jimenez, J. L.: Field-deployable, high-resolution, Time-of-Flight Aerosol Mass Spectrometer, *Anal. Chem.*, 78, 8281–8289, 2006.
- Engeln, R., Berden, G., Peeters, R., and Meijer, G.: Cavity enhanced absorption and cavity enhanced magnetic rotation spectroscopy, *Rev. Sci. Instr.*, 69, 3763–3769, 1998.
- Ervens, B., Feingold, G., Frost, G. J., and Kreidenweis, S. M.: A modeling study of aqueous production of dicarboxylic acids: 1. Chemical pathways and speciated organic mass production, *J. Geophys. Res.*, 109, D15205, doi:10.1029/2003JD004387, 2004.
- Faulhaber, A. E., Thomas, B. M., Jimenez, J. L., Jayne, J., Worsnop, D. R., and Ziemann, P. J.: Characterization of a thermodenuder-particle beam mass spectrometer system for the study of organic aerosol volatility and composition, *Atmos. Meas. Techn.*, 2, 15–31, doi:10.5194/amt-2-15-2009, 2009.
- Fiedler, S. E., Hese, A., and Ruth, A. A.: Incoherent broad-band cavity-enhanced absorption spectroscopy of liquids, *Rev. Sci. Instrum.*, 76, 023107, 2005.
- Fiedler, S. E., Hese, A., and Ruth, A. A.: Incoherent broad-band cavity-enhanced absorption spectroscopy, *Chem. Phys. Lett.*, 371, 2003.
- Finlayson-Pitts, B. J. and Pitts, J. N.: *Chemistry of the upper and lower atmosphere: Theory, experiments, and applications*, Academic Press, San Diego, CA, USA, 1999.
- Fu, T.-M., Jacob, D. J., Wittrock, F., Burrows, J. P., Vrekoussis, M., and Henze, D. K.: Global budgets of atmospheric glyoxal and methylglyoxal and implications for formation of secondary organic aerosols, *J. Geophys. Res.*, 113, D15303, doi:10.1029/2007JD009505, 2008.
- Galloway, M. M., Chhabra, P., Chan, A. W. H., Surratt, J. D., Flagan, R. C., Seinfeld, J. H., and Keutsch, F. N.: Glyoxal uptake on ammonium sulphate seed aerosol: reaction products and reversibility of uptake under dark and irradiated conditions, *Atmos. Chem. Phys.*, 9, 3331–3345, doi:10.5194/acp-9-3331-2009, 2009.

- Galloway, M. M., Loza, C. L., Chhabra, P. S., Chan, A. W. H., Yee, L. D., Seinfeld, J. H., and Keutsch, F. N.: Analysis of photochemical and dark glyoxal uptake: Implications for SOA formation, *Geophys. Res. Lett.*, 38, L17811, doi:10.1029/2011gl048514, 2011.
- Hallquist, M., Wenger, J. C., Baltensperger, U., Rudich, Y., Simpson, D., Claeys, M., Dommen, J., Donahue, N. M., George, C., Goldstein, A. H., Hamilton, J. F., Herrmann, H., Hoffmann, T., Iinuma, Y., Jang, M., Jenkin, M., Jimenes, J. L., Kiendler-Scharr, A., Maenhaut, W., McFiggans, G., Mentel, T. F., Monod, A., Prevot, A. S., Seinfeld, J. H., Surratt, J. D., Szmigielski, R., and Willdt, J.: The formation, properties and impact of secondary organic aerosol: current and emerging issues, *Atmos. Chem. Phys.*, 9, 5155–5236, doi:10.5194/acp-9-5155-2009, 2009.
- Hamilton, J. F., Webb, P. J., Lewis, A. C., and Reviejo, M. M.: Quantifying small molecules in secondary organic aerosol formation during the photo-oxidation of toluene with hydroxyl radicals, *Atmos. Environ.*, 39, 7263–7275, 2005.
- Healy, R. M., Wenger, J. C., Metzger, A., Duplissy, J., Kalberer, M., and Dommen, J.: Gas/particle partitioning of carbonyls in the photooxidation of isoprene and 1,3,5-trimethylbenzene, *Atmos. Chem. Phys.*, 8, 3215–3230, doi:10.5194/acp-8-3215-2008, 2008.
- Hurley, M. D., Sokolov, O., Wallington, T. J., Takekawa, H., Karasawa, M., and Klotz, B.: Organic aerosol formation during the atmospheric degradation of toluene, *Environ. Sci. Technol.*, 35, 1358–1366, 2001.
- Ip, H. S. S., Huang, X. H. H., and Yu, J. Z.: Effective Henry's law constants of glyoxal, glyoxylic acid, and glycolic acid, *Geophys. Res. Lett.*, 36, L01802, doi:10.1029/2008GL036212, 2009.
- Jang, M. and Kamens, R. M.: Atmospheric Secondary Aerosol Formation by Heterogeneous Reactions of Aldehydes in the Presence of a Sulfuric Acid Aerosol Catalyst, *Environ. Sci. Technol.*, 35, 4758–4766, 10.1021/es010790s, 2001.
- Jayne, J. T., Leard, D. C., Zhang, X., Davidovits, P., Smith, K. A., Kolb, C. E., and Worsnop, D. R.: Development of an Aerosol Mass Spectrometer for size and composition analysis of submicron particles, *Aerosol Sci. Technol.*, 33, 49–70, 2000.
- Jimenez, J. L., Canagaratna, M. R., Donahue, N. M., Prevot, A. S. H., Zhang, Q., Kroll, J. H., DeCarlo, P. F., Allan, J. D., Coe, H., Ng, N. L., Aiken, A. C., Docherty, K. S., Ulbrich, I. M., Grieshop, A. P., Robinson, A. L., Duplissy, J., Smith, J. D., Wilson, K. R., Lanz, V. A., Hueglin, C., Sun, Y. L., Tian, J., Laaksonen, A., Raatikainen, T., Vaattovaara, P., Ehn, M., Kulmala, M., Tomlinson, J. M., Collins, D. R., Cubison, M. J., Dunlea, E. J., Huffman, J. A., Onasch, T. B., Alfarra, M. R., Williams, P. I., Bower, K., Kondo, Y., Schneider, J., Drewnick, F., Borrmann, S., Weimer, S., Demerjian, K., Salcedo, D., Cottrell, L., Griffin, R. J., Takami, A., Miyoshi, T., Hatakeyama, S., Shimono, A., Sun, J. Y., Zhang, Y. M., Dzepina, K., Kimmel, J. R., Sueper, D., Jayne, J. T., Herndon, S. C., Trimborn, A. M., Williams, L. R., Wood, E. C., Middlebrook, A. M., Kolb, C. E., Baltensperger, U., and Worsnop, D. R.: Evolution of organic aerosols in the atmosphere, *Science*, 326, 1525–1529, 2009.
- Johnson, D., Jenkin, M., Wirtz, K., and Martin-Reviejo, M.: Simulating the formation of secondary organic aerosol from the photooxidation of toluene, *Environ. Chem.*, 1, 150–165, 2004.
- Johnson, D., Jenkin, M. E., Wirtz, K., and Martin-Reviejo, M.: Simulating the formation of secondary organic aerosol from the photooxidation of aromatics hydrocarbons, *Environ. Chem.*, 2, 35–48, 2005.
- Kalberer, M., Paulsen, D., Sax, M., Steinbacher, M., Dommen, J., Prevot, A. S., Fisseha, R., Weingartner, E., Frankevich, V., Zenobi, R., and Baltensperger, U.: Identification of polymers as major components of atmospheric organic aerosols, *Science*, 303, 1659–1662, 2004.
- Kalberer, M., Sax, M., and Samburova, V.: Molecular size evolution of oligomers in organic aerosols collected in urban atmospheres and generated in a smog chamber, *Environ. Sci. Technol.*, 40, 5917–5922, 2006.
- Kamens, R. M., Zhang, H., Chen, E. H., Zhou, Y., Parikh, H. M., Wilson, R. L., Galloway, K. E., and Rosen, E. P.: Secondary organic aerosol formation from toluene in an atmospheric hydrocarbon mixture: Water and particle seed effects, *Atmos. Environ.*, 45, 2324–2334, 2011.
- Kroll, J. H., Ng, N. L., Murphy, S. M., Varutbangkul, V., Flagan, R. C., and Seinfeld, J. H.: Chamber studies of secondary organic aerosol growth by reactive uptake of simple carbonyl compounds, *J. Geophys. Res.*, 110, D23207, doi:10.1029/2005JD006004, 2005.
- Langridge, J. M., Ball, S. M., and Jones, R. L.: A compact broadband cavity enhanced absorption spectrometer for detection of atmospheric NO<sub>2</sub> using light emitting diodes, *Analyst*, 131, 916–922, 2006.
- Liggio, J., Li, S.-M., and McLaren, R.: Heterogeneous reactions of glyoxal on particulate matter: identification of acetals and sulfate esters, *Environ. Sci. Technol.*, 39, 1532–1541, 2005a.
- Liggio, J., Li, S.-M., and McLaren, R.: Reactive uptake of glyoxal by particulate matter, *J. Geophys. Res.*, 110, D10304, doi:10.1029/2004JD005113, 2005b.
- Lim, Y. B., Tan, Y., Perri, M. J., Seitzinger, S. P., and Turpin, B. J.: Aqueous chemistry and its role in secondary organic aerosol (SOA) formation, *Atmospheric Chemistry and Physics*, 10, 10521–10539, doi:10.5194/acp-10-10521-2010, 2010.
- Loza, C. L., Chan, A. W. H., Galloway, M. M., Keutsch, F. N., Flagan, R. C., and Seinfeld, J. H.: Characterization of vapor wall loss in laboratory chambers, *Environ. Sci. Technol.*, 44, 5074–5078, 2010.
- Nakao, S., Clark, C., Tang, P., Sato, K., and Cocker III, D.: Secondary organic aerosol formation from phenolic compounds in the absence of NO<sub>x</sub>, *Atmos. Chem. Phys.*, 11, 10649–10660, 10, <http://www.atmos-chem-phys.net/11/10649/10/5194/acp-11-10649-2011>, 2011a.
- Nakao, S., Shrivastava, M., Nguyen, A., Jung, H., and Cocker, D.: Interpretation of Secondary Organic Aerosol Formation from Diesel Exhaust Photooxidation in an Environmental Chamber, *Aerosol Sci. Technol.*, 45, 954–962, 2011b.
- Nenes, A., Pandis, S. N., and Pilinis, C.: ISORROPIA: A New Thermodynamic Equilibrium Model for Multiphase Multicomponent Inorganic Aerosols, *Aquat. Geochem.*, 4, 123–152, doi:10.1023/a:1009604003981, 1998.
- Ng, N. L., Kroll, J. H., Chan, A. W. H., Chhabra, P., Flagan, R. C., and Seinfeld, J. H.: Secondary organic aerosol formation from m-xylene, toluene, and benzene, *Atmos. Chem. Phys.*, 7, 3909–3922, doi:10.5194/acp-7-3909-2007, 2007.
- Nozière, B., Dziedzic, P., and Córdoba, A.: Products and Kinetics of the Liquid-Phase Reaction of Glyoxal Catalyzed by

- Ammonium Ions ( $\text{NH}_4^+$ ), *J. Phys. Chem. A*, 113, 231–237, doi:10.1021/jp8078293, 2008.
- Odum, J. R., Hoffman, T., Bowman, F., Collins, D., Flagan, R. C., and Seinfeld, J. H.: Gas/particle partitioning and secondary organic aerosol yields, *Environ. Sci. Technol.*, 30, 2580–2585, 1996.
- Olariu, R. I., Klotz, B., Barnes, I., Becker, K. H., and Mocanu, R.: FT-IR study of the ring-retaining products from the reaction of OH radicals with phenol, o-, m-, and p-cresol, *Atmos. Environ.*, 36, 3685–3697, 2002.
- Pankow, J. F.: An absorption model of gas/particle partitioning of organic compounds in the atmosphere, *Atmos. Environ.*, 28, 185–188, 1994.
- Paul, J. B., Lapson, L., and Anderson, J. G.: Ultrasensitive absorption spectroscopy with a high-finesse optical cavity and off-axis alignment, *Appl. Optics*, 40, 4904–4910, 2001.
- Prenni, A. J., Petters, M. D., Kreidenweis, S. M., DeMott, P. J., and Ziemann, P. J.: Cloud droplet activation of secondary organic aerosol, *J. Geophys. Res.*, 112, D10223, doi:10.1029/2006JD007963, 2007.
- Qi, L., Nakao, S., Malloy, Q., Warren, B., and Cocker, D. R.: Can secondary organic aerosol formed in an atmospheric simulation chamber continuously age?, *Atmos. Environ.*, 44, 2990–2996, 2010a.
- Qi, L., Nakao, S., Tang, P., and Cocker III, D. R.: Temperature effect on physical and chemical properties of secondary organic aerosol from m-xylene photooxidation, *Atmos. Chem. Phys.*, 10, 3847–3854, doi:10.5194/acp-10-3847-2010, 2010b.
- Rader, D. J. and McMurry, P. H.: Application of the Tandem Differential Mobility Analyzer to studies of droplet growth or evaporation, *J. Aerosol Sci.*, 17, 771–787, 1986.
- Sato, K., Hatakeyama, S., and Imamura, T.: Secondary organic aerosol formation during the photooxidation of toluene: NO<sub>x</sub> dependence of chemical composition, *J. Phys. Chem. A*, 111, 9796–9808, 2007.
- Seinfeld, J. H. and Pandis, S. N.: *Atmospheric Chemistry and Physics: From Air Pollution to Climate Change* — 2nd ed., A Wiley-Interscience publication, New Jersey, USA, 2006.
- Smith, M. L., Kuwata, M., and Martin, S. T.: Secondary Organic Material Produced by the Dark Ozonolysis of  $\alpha$ -Pinene Minimally Affects the Deliquescence and Efflorescence of Ammonium Sulfate, *Aerosol Sci. Technol.*, 45, 244–261, 2011.
- Sun, Y. L., Zhang, Q., Anastasio, C., and Sun, J.: Insights into secondary organic aerosol formed via aqueous-phase reactions of phenolic compounds based on high resolution mass spectrometry, *Atmos. Chem. Phys.*, 10, 4809–4822, doi:10.5194/acp-10-4809-2010, 2010.
- Surrat, J. D., Kroll, J. H., Kleinsienst, T. E., Edney, E. O., Claeys, M., Sorooshian, A., Ng, N. L., Offenberg, J. H., Lewandowski, M., Jaoui, M., Jaouri, R., Flagan, R. C., and Seinfeld, J. H.: Evidence for organosulfates in secondary organic aerosol, *Environ. Sci. Technol.*, 41, 517–527, 2007.
- Takekawa, H., Minoura, H., and Yamazaki, S.: Temperature dependence of secondary organic aerosol formation by photo-oxidation of hydrocarbons, *Atmos. Environ.*, 37, 3413–3424, 2003.
- Tolocka, M. P., Jang, M., Ginter, J. M., Cox, F. J., Kamens, R. M., and Johnston, M. V.: Formation of oligomers in secondary organic aerosol, *Environ. Sci. Technol.*, 38, 1428–1434, 2004.
- Volkamer, R., Klotz, B., Barnes, I., Imamura, T., and Washida, N.: OH-initiated oxidation of benzene Part I. Phenol formation under atmospheric conditions, *Phys. Chem. Chem. Phys.*, 4, 1598–1610, 2002.
- Volkamer, R., Spietz, P., Burrows, J., and Platt, U.: High-resolution absorption cross-section of glyoxal in the UV-vis and IR spectral ranges, *J. Photochem. Photobiol. A-Chem.*, 172, 35–46, 2005.
- Volkamer, R., Martini, F. S., Molina, L. T., Salcedo, D., Jimenez, J. L., and Molina, M. J.: A missing sink for gas-phase glyoxal in Mexico city: Formation of secondary organic aerosol, *Geophys. Res. Lett.*, 34, L19807, doi:10.1029/2007GL030752, 2007.
- Volkamer, R., Ziemann, P. J., and Molina, L. T.: Secondary organic aerosol formation from acetylene ( $\text{C}_2\text{H}_2$ ): seed effect on SOA yields due to organic photochemistry in the aerosol aqueous phase, *Atmos. Chem. Phys.*, 9, 1907–1928, doi:10.5194/acp-9-1907-2009, 2009.
- Warren, B., Malloy, Q., Yee, L. D., and Cocker, D. R.: Secondary organic aerosol formation from cyclohexene ozonolysis in the presence of water vapor and dissolved salts, *Atmospheric Environment*, 43, 1789–1795, 2009.
- Washenfelder, R. A., Langford, A. O., Fuchs, H., and Brown, S. S.: Measurement of glyoxal using an incoherent broadband cavity enhanced absorption spectrometer, *Atmos. Chem. Phys.*, 8, 7779–7793, doi:10.5194/acp-8-7779-2008, 2008.
- Washenfelder, R. A., A. O. Langford, H. Fuchs, and S. S. Brown: Measurements of glyoxal using an incoherent broadband cavity enhanced absorption spectrometer, *Atmos. Chem. Phys.*, 8, 7779–7793, doi:10.5194/acp-8-7779-2008, 2008.
- Zhou, Y., Zhang, H., Parikh, H. M., Chen, E. H., Rattanavaraha, W., Rosen, E. P., Wang, W., and Kamens, R. M.: Secondary Organic Aerosol Formation from Xylenes and Mixtures of Toluene and Xylenes in an Atmospheric Urban Hydrocarbon Mixture: Water and Particle Seed Effects (II), *Atmos. Environ.*, 45, 3882–3890, 2011.